GIScience & Remote Sensing

ISSN: (Print) (Online) Journal homepage: https://www.tandfonline.com/loi/tgrs20

Contribution of anthropogenic consolidation processes to subsidence phenomena from multi-temporal DInSAR: a GIS-based approach

Francesca Grassi, Francesco Mancini, Elisa Bassoli & Loris Vincenzi

To cite this article: Francesca Grassi, Francesco Mancini, Elisa Bassoli & Loris Vincenzi (2022) Contribution of anthropogenic consolidation processes to subsidence phenomena from multi-temporal DInSAR: a GIS-based approach, GIScience & Remote Sensing, 59:1, 1901-1917, DOI: 10.1080/15481603.2022.2143683

To link to this article: https://doi.org/10.1080/15481603.2022.2143683

Published online: 10 Nov 2022.

GISCIENCE & REMOTE SENSING
2022, VOL. 59, NO. 1, 1901–1917
https://doi.org/10.1080/15481603.2022.2143683

Taylor & Francis
Taylor & Francis Group

Contribution of anthropogenic consolidation processes to subsidence phenomena from multi-temporal DInSAR: a GIS-based approach

Francesca Grassi, Francesco Mancini, Elisa Bassoli and Loris Vincenzi

Department of Engineering "Enzo Ferrari," University of Modena and Reggio Emilia, Modena, Italy

ABSTRACT

The paper introduces an approach based on the combination of multi-temporal Differential Interferometric Synthetic Aperture Radar and geographical information systems analysis to investigate and separate several contributions to subsidence phenomena over the municipality of Ravenna (Emilia Romagna, Italy). In particular, the relationship between displacements detected over built environment and consolidation processes after construction was assessed and filtered out from the subsidence map to quantify the local overestimation of subsidence phenomena due to the mentioned processes. It requires descriptive attributes related to the age of construction and intended uses. The outcomes of the present study highlight ground consolidation processes that seem to be active over areas settled in the last 30 years with a component contributing to vertical rates up to 3 mm/yr. Such contribution represents the 20% of the cumulative displacements reported for coastal villages where different sources of subsidence increase the vulnerability to coastal erosion. We discuss the contribution of consolidation processes over a couple of recently settled areas to separate among contributions and avoid the misinterpretation of effects due to other anthropogenic sources of subsidence.

ARTICLE HISTORY
Received 19 July 2022
Accepted 19 October 2022

KEYWORDS
mt-InSAR; Sentinel-1; consolidation processes; subsidence components

Introduction

Investigations about natural and anthropogenic components of subsidence by satellite radar interferometry have been widely presented in the scientific literature (Gabriel, Goldstein, and Zebker 1989; Ferretti, Prati, and Rocca 2000; Teatini et al. 2006; Stramondo et al. 2007; Bitelli et al. 2015; Del Soldato et al. 2018; Ghorbanzadeh et al. 2018; Cian, Delgado Blasco, and Carrera 2019; Delgado Blasco et al. 2019; Mancini, Grassi, and Cenni 2021; Li et al. 2022) thanks to the ability of the technique to detect the displacement of targets at the ground along the line of sight (LOS) direction at a high accuracy level (1–2 mm/yr) and spatial resolutions up to few meters of the more recent SAR missions (e.g. Sentinel-1, Radarsat, COSMO-SkyMed, and TerraSAR-X) (Casu, Manzo, and Lanari 2006; Crosetto et al. 2016). More recently, few papers focussed on GIS-based post analyses of SAR products for advanced applications have been reported (Qiu et al. 2021; Radman, Akhoondzadeh, and Hosseiny 2021; Barra et al. 2022). As additional advantage of the SAR interferometry, the temporal and spatial analysis of the detected displacements provides further insights into the deformation phenomena and their possible natural and anthropogenic drivers (Carminati and Martinelli 2002; Teatini, Tosi, and Strozzi 2011; Tosi, Teatini, and Strozzi 2013). Ground deformation phenomena were initially investigated thanks to interferograms produced by the Differential Interferometric Synthetic Aperture Radar (DInSAR) technique based on three, or four, satellite passes. Today, ground deformation processes are more frequently studied by persistent scatterer interferometry (PSI), homogeneous distributed scatterer interferometry (HDSI), and small baseline subsets (SBAS). PSI (Ferretti, Prati, and Rocca 2000, 2001; Hooper et al. 2004; Hooper, Segall, and Zebker 2007), HDSI (Ferretti et al. 2011) and SBAS (Berardino et al. 2002; Lanari et al. 2004) could refer to different statistical approaches to select stable and coherent targets and find the velocity of these scatterers from the time series of displacement occurring between successive satellite passes. However, whatever methodology is selected, the mentioned approaches allow to compute the displacement of a multitude of scatterers with respect to a reference position and a reference epoch. Therefore, the absolute velocity of one or more points within the studied area is

CONTACT Francesco Mancini francesco.mancini@unimore.it

required to transpose the relative displacement field into absolute values in a defined reference frame. Due to the wavelengths employed in the SAR systems (typically, the C and X bands), the methodology is particularly suited for the detection of ground deformation phenomena occurring at very low rates (few mm/year). Major limitations can be related to spatial and temporal decorrelation phenomena and the ability to detect only a minor part of the actual displacements occurring at the ground due to the slant-oriented acquisition geometry. Depending on the incidence angle, satellite interferometry is mainly sensitive toward displacement occurring along the vertical and, at less extent, in the East–West directions (Hanssen 2001; Samieie-Esfahany et al. 2009). The abovementioned reasons make the SAR interferometry complemented by few global navigation satellite systems (GNSS) observations a powerful method to detect subsidence phenomena at the desired spatial scale (Farolfi, Bianchini, and Casagli 2019).

Very often, subsidence phenomena are investigated over areas where major cities have been developed and, furthermore, the built environment is particularly suited for analysis based on persistent scatterers (PS). However, the different natural and/or anthropogenic sources of subsidence in settled areas cannot be distinguished, being the measured displacement of scatterers the overall displacement occurring at the ground. Different contributions compose the overall displacement, such as long-time trends of natural compaction processes of fine-grained sediments, groundwater table depth variation in response to pumping for industrial and drinking purposes (Stramondo et al. 2008; Abidin et al. 2011; Dang et al. 2014; Chen et al. 2015; Qin and Perissin 2015; Lyu et al. 2020; Bui et al. 2021), gas storage/exploitation or activities related to oil industries (Bertoni et al. 1995; Teatini et al. 2005; Simeoni et al. 2017; Mancini, Grassi, and Cenni 2021) mining activities (Samsonov, d'Oreye, and Smets 2013; Wang et al. 2022). Moreover, the consolidation processes due to recently built structure load could further affect the subsidence mapping, in particular for studies devoted to the analysis of ground deformation phenomena at local scale (superficial effects of groundwater and gas reservoir exploitation, tunneling, excavation), where the spatial deformation pattern could be strongly affected by the consolidation processes for more than two decades (Chen and Richard Liew 2002). With reference to consolidation processes after construction, Ketelaar et al. (2020) and Van Leijen, Marel, and Hanssen (2021) proposed a method for the classification of scatterers to better distinguish between deep and shallow processes; in these works the targets are separated into two groups (i.e. the well-founded objects sensitive to deep processes only and those sensitive to the total ground motion) exploiting a criterion based on the relative scatterer height with respect to the terrain height. However, in the present paper, due to the stratigraphic setting, that will be further discussed, the building displacements are sensitive both to superficial and shallow processes, and the approach proposed in the mentioned papers cannot be adopted.

The relationship between subsidence and possible causal factors has been reported in particular for megacities around the world and the attempt to separate natural and anthropogenic components of subsidence has been limited to further investigation on imposed load and the construction age of the buildings (Tang et al. 2008; Xu et al. 2012; Solari et al. 2016). However, a quantitative separation between natural and anthropogenic components of subsidence into possible contributions is still an open problem requiring a more advanced integration between results provided by SAR interferometry and available geospatial datasets. In particular, the quantification and separation of target displacements detected by SAR interferometry, which are not due to common subsidence phenomena, provides a better understanding of the specific phenomenon of interest and avoid the overestimation and misinterpretation of subsidence trends because of the influence of unexpected factors, such as the consolidation processes of recent settlements. For this purpose, an approach that integrates geographical information systems (GIS)-based spatial analysis and measurements from multi-temporal InSAR could be employed. However, the application of these approaches for consolidation process assessment is still in a superficial stage. A deeper integration with the GIS environment was proposed by Tomás et al. (2019) and Macchiarulo et al. (2022) who adopted clustering analyses to define structural deformation processes and by Scivetti et al. (2021) who investigated the relation between LOS velocities and urban growth at the neighborhood scale and geomorphologic features. In the attempt to better understand the

anthropogenic processes affecting subsidence studies by integrating GIS data about the built environment, Fiaschi et al. (2017) introduced the contribution of the land use changes in the interpretation of land subsidence retrieved from the analysis of ERS-1/2 and TerraSAR-X images. A correlation between increasing values of subsidence rates and a land use change to construction unit was also shown and interpreted as an effect of sediment compaction caused by the load of the newly constructed building.

In this paper, we introduce an approach based on the combination of SAR interferometry and spatial analysis by GIS to improve the separation among natural and anthropogenic components of subsidence over the municipality of Ravenna (Italy), a 650 - km^2 wide study area in which subsidence phenomena can be observed. In particular, we focused on the use of large dataset to quantify the displacement of targets due to external factors, such as consolidation processes under building loads and their dependency from the age of construction for selected intended uses. To this aim, displacements obtained from a processing workflow based on Sentinel Application Platform (SNAP) and the Stanford Method for Persistent Scatterers (StaMPS) and ascending and descending Sentinel-1 data have been combined with GIS geometric and descriptive data and GNSS observations.

Study area

The present study investigates the area of the municipality of Ravenna (Emilia-Romagna, Italy), a lowland belonging to the eastern area of the alluvial Po plain and faced to the Adriatic Sea. The area is characterized by coastal zones with elevation not exceeding 2 meters above sea level (a.s.l.), with large portions below mean sea level, and the presence of land reclamation, wet areas, and salt marshes (see Figure 1). Due to a combination of anthropogenic and natural geological processes, in the last decade the land has been subjected to cumulative rates of subsidence up to 5 mm/yr in Ravenna and inner sectors and around 15 mm/yr over limited extent of coastal stretches (subsidence rates from InSAR as provided by ARPAe, Regional Agency for Prevention, Environment, and

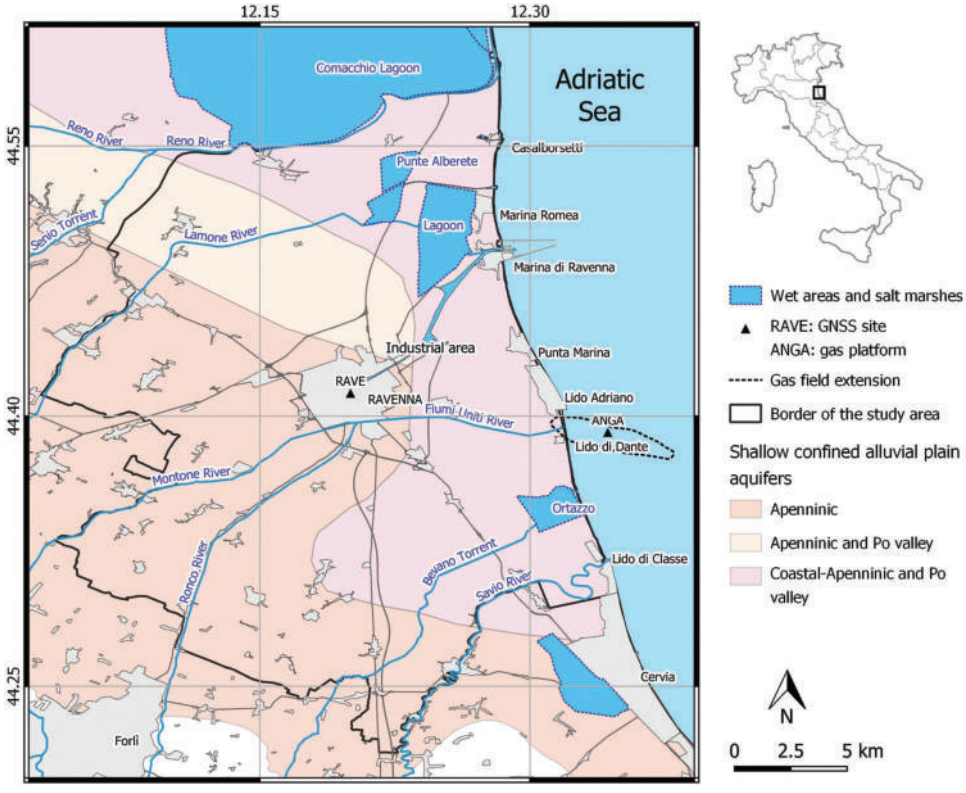

Figure 1. Map of the study area with borders of the municipality of Ravenna (Emilia Romagna, Italy), the extension of the gas field and the shallow confined aquifers. ANGA: Angela and Angelina offshore platforms for natural gas exploitation; RAVE: Continuous GNSS station.

Energy of Emilia-Romagna, to the year 2016; see ARPAe 2018, https://arpae.it/cartografia/, Polcari et al. 2022). Natural and anthropogenic components of subsidence in the study areas have been deeply investigated by several authors. Rates of natural land subsidence arise from the combination of deep downward tectonic movement (Carminati, Doglioni, and Scrocca 2003) and the compaction of recent Holocene (Quaternary) sediments (Teatini, Tosi, and Strozzi 2011). Gambolati and Teatini (1998) estimate a natural subsidence rate in the area of about 2–3 mm/yr over the last 2,500 years and Antonellini et al. (2019) assigned 0.9 mm/yr of the total estimate to primary consolidation processes of the fine-grained prodelta levels. In the area, the anthropogenic land subsidence was caused by the fast industrial development occurred in the years after the World War II and is mainly due to groundwater pumping from shallow and deep aquifers and to gas exploitation from Plio-Pleistocene inland and offshore reservoirs (Bertoni et al. 1995; Teatini et al. 2005); Figure 1 shows the extent of the shallow aquifers and the Angela and Angelina offshore reservoir. These factors caused an intense subsidence that reached the value of 110 mm/yr during the 1970s. The actions undertaken in the late 1970s and 1980s by the municipalities reduced the groundwater pumping, thus reducing the subsidence rate to the values registered in the first half of the 20th century (Teatini et al. 2005, 2006). During the last two decades, the mainland appeared to be stable or slightly subsiding, while part of the coastal areas still present a subsidence of about 10 mm/yr. In particular, some criticalities still remain in the area of Lido Adriano, Lido di Dante and in the industrial area between Marina di Ravenna and the city center (Teatini et al. 2005). These trends were confirmed by the DInSAR analyses carried out by Antoncecchi et al. (2021) in the periods 1995–2010 and 2015–2018.

The total amount of land subsidence, in addition to modern trends in sea level rise up to 2.2 ± 1.3 mm/yr (Cerenzia et al. 2016), made the coastal areas strongly vulnerable to erosive processes and open problems connected to engineering works for coastal protection of the settlements (Sytnik and Stecchi 2014).

Available data and processing workflow

The present paper integrates displacement from the implemented PSI method and a GIS dataset of the built environment. The interferometric processing is based on the combination of open-source routines from SNAP, StaMPS, the Toolbox for Reducing Atmospheric InSAR Noise (TRAIN), and MATLAB routines introduced by the authors for the calibration and decomposition of the dual-orbit dataset.

Sentinel-1A and -1B radar dataset

Sentinel-1 (S1) Single Look Complex (SLC) data acquired with the Interferometric Wide (IW) mode, with a resolution of 20 m in the azimuth and 5 m in the range directions, were downloaded from the Sentinel Scientific Data Hub (scihub.copernicus.eu) and processed with an open-source procedure. The resolution achieved by the IW mode makes the S1 SLC IW data particularly suitable for land deformation studies; moreover, the high incidence angles of the selected acquisitions (reported in Figure 2) ensure a greater sensitivity to horizontal component in the decomposition procedure. The extent and details on the interferometric ascending and descending datasets can be found in Figure 2.

Interferometric data processing

The full chain of SAR data processing was performed using a combination of SNAP (provided by the European Space Agency, ESA) and StaMPS open-source tools (developed by Stanford University, University of Iceland, Delft University, and University of Leeds). In particular, SNAP was used to generate the stack of interferograms and remove the topographic phase. SNAP contains all the necessary tools for the processing of ESA (S1, ERS-1, ERS-2, Envisat) and other space agencies (e.g. COSMO SkyMed) radar mission data and ensures the integration with the StaMPS package. The StaMPS package provides PSI time series analysis from the stack of interferograms and extracts ground displacements also for non-steady deformation (Hooper et al. 2012, 2018). At the end of the StaMPS processing, the removal of the atmospheric contribution was performed by the TRAIN module, implemented in StaMPS (Bekaert, Hooper, and Wright 2015; Bekaert, Walters et al. 2015). Finally, the last part of the processing (i.e. the calibration, decomposition, and, eventually, the validation steps) was performed with MATLAB routines written by the authors. The validation step of the SAR

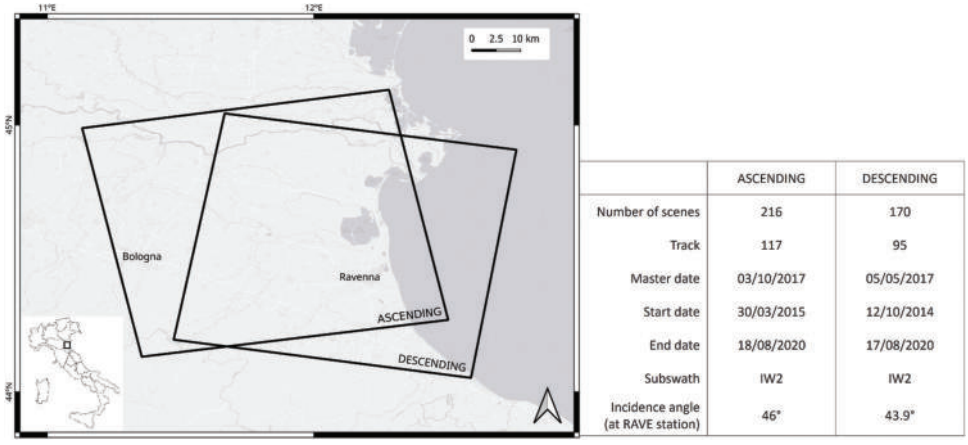

	ASCENDING	DESCENDING
Number of scenes	216	170
Track	117	95
Master date	03/10/2017	05/05/2017
Start date	30/03/2015	12/10/2014
End date	18/08/2020	17/08/2020
Subswath	IW2	IW2
Incidence angle (at RAVE station)	46°	43.9°

Figure 2. Extension and details of the processed Sentinel-1 ascending and descending dataset.

results using GNSS observations is omitted in the present work; however, the adopted procedure was previously validated in Mancini, Grassi, and Cenni (2021). The whole processing procedure is presented in Figure 3 (see Mancini, Grassi, and Cenni 2021 for a comprehensive description of the adopted workflow).

The interferometric processing performed in SNAP includes firstly the selection of the optimal master image (Zebker and Villasenor 1992), the splitting, and the orbital correction of the products. Secondly, the coregistration of the products, the deburst, the generation of the interferograms, and the removal of the topographic phase component using the shuttle radar topography mission (SRTM) 3 arcseconds are performed. Lastly, the folders for the StaMPS processing are generated from the stack of and the debursted products and the stack of the interferograms without the topographic phase (i.e. the StaMPS export step).

The PSI processing performed in StaMPS starts with the setting of the processing parameters using the appropriate script. In the present work, we adopted an amplitude dispersion $D_a = 0.40$, a number of overlapping pixels in the azimuth (n_a) and range direction (n_r) of 200 and 50, respectively. The patch dimensions in azimuth and range were set to 3. Then, the complete workflow of the processing was carried out following the eight steps of the StaMPS procedure (i.e. data loading, phase noise estimation, persistent scatterer selection, persistent scatterer weeding, phase correction, phase unwrapping, spatially correlated look angle error estimation, estimation of other spatially correlated noise) as described in Hooper et al. (2018). Once the StaMPS workflow processing is completed, the TRAIN correction can be performed;

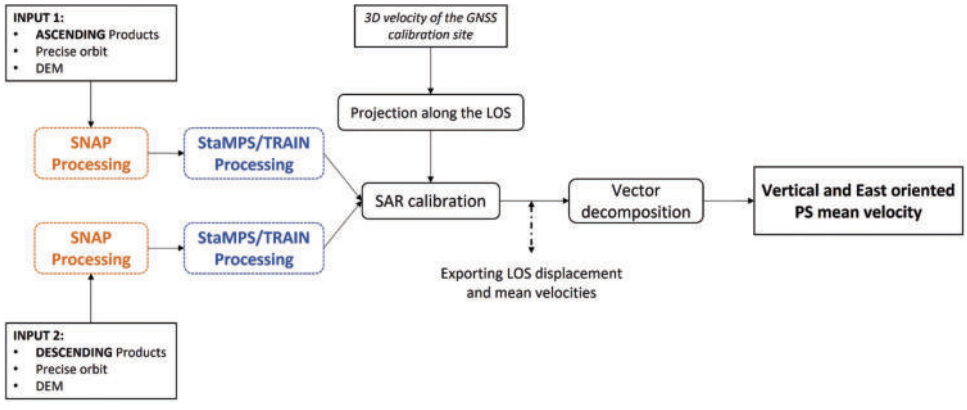

Figure 3. The SNAP–StaMPS workflow adopted for the processing of S1 data (from Mancini, Grassi, and Cenni 2021 with modifications).

among the available models, the phase-based linear was adopted in the present work.

A phase-based linear correction can be performed. To refer displacements to a global reference frame, the StaMPS provides the chance to select a reference point/area with known velocityfor instance, where continuous GNSS (CGNSS) sites are available. For this purpose, the velocity of the reference site is projected along the local LOS for both the orbits; the velocity components along the vertical (UP), North (N), and East (E) directions are obtained by (Hanssen 2001; Samieie-Esfahany et al. 2009):

$$\begin{aligned} v_{LOS,GNSS} = {} & v_{UP,GNSS}\cos(\theta_{inc}) \\ & - \sin(\theta_{inc})\left(v_{N,GNSS}\cos\left(\alpha_H - \frac{3\pi}{2}\right)\right. \\ & \left. + v_{E,GNSS}\sin\left(\alpha_H - \frac{3\pi}{2}\right)\right) \end{aligned} \quad (1)$$

where θ_{inc} is the incidence angle, α_H is the satellite orbit heading angle, $v_{UP,GNSS}$, $v_{N,GNSS}$ and $v_{E,GNSS}$ are the mean velocity components in the vertical, North, and East directions, respectively. Using the GNSS velocities projected along the LOS, the SAR displacements can be referred to a global reference frame (calibration step).

Successively, the decomposition analysis can be performed. Given the low sensitivity of the method along the North–South direction (Hanssen 2001), only velocities along the Up and East directions were derived from the ascending and descending calibrated LOS velocities (v_{LOS}^{ASC} and v_{LOS}^{DESC}) by the formula:

$$\begin{bmatrix} v_{UP} \\ v_{EAST} \end{bmatrix} = A^{-1} \cdot \begin{bmatrix} v_{LOS}^{ASC} \\ v_{LOS}^{DESC} \end{bmatrix} \quad (2)$$

where

$$A = \begin{bmatrix} \cos(\theta_{inc,asc}) & \sin(\theta_{inc,asc})\cos(\alpha_{H,asc}) \\ \cos(\theta_{inc,desc}) & -\sin(\theta_{inc,desc})\cos(\alpha_{H,desc}) \end{bmatrix} \quad (3)$$

It is worth noting that the value of $\theta_{inc,asc}$ is negative because of its counter clockwise counting.

GIS dataset

The GIS dataset is composed of information relating to the urbanized and natural environment. These data are available in the geographic repositories of the Emilia Romagna Region and the Municipality of Ravenna. The dataset is available through the open-source data management system CKAN (Comprehensive Knowledge Archive Network) developed by Open Knowledge Foundation to publish, share, and use open data by handling geospatial ArcGIS portals and major metadata schemas. The layers representing the built environment are available as shapefiles (.shp) and FeatureCollections in geoJSON (.JSON) formats. Besides the geometric entities included in the layers, detailed descriptive attributes fundamental in the successive spatial analysis have also been provided. In particular, this work used the information layers relating to the classes of buildings and constructions. In this layer, 60,700 buildings are represented with additional fields containing information used in the present study such as the intended use, year of construction, subsequent maintenance, restructuring interventions, and many others. Among the list of intended uses listed in the attributes of the dataset, civil and industrial have been considered in the present study.

Results

The combined SNAP-StaMPS processing of dual orbit S1 SLC images produced a geocoded LOS-oriented velocity map over the study area. Pixels characterized by $D_a > 0.4$ were filtered out to scatterers that showed low temporal coherence. The local deformation trend provided by Bonetti et al. (2022) was taken into account to refer the LOS velocities to a common reference frame. In particular, the continuous GNSS station named RAVE was chosen to guarantee a reliable constraint to the global reference frame. Moreover, as can be seen from Figure 1, the selected GNSS station is located in the center of the study area. The velocities at the RAVE site refer to a period of observation that overlaps with the interferometric dataset and amounts at: V_{UP} = –4.6 mm/yr, V_{EAST} = 1.0 mm/yr, and V_N = 3.1 mm/yr (the European Terrestrial Reference Frame is adopted to remove the Eurasian plate motion). Similar rates of subsidence have been reported by ARPAe (ARPAe 2018). After projecting the GNSS velocities along the ascending and descending LOS directions, the LOS-oriented velocity maps of the study area were obtained (Figure 4).

Starting from the results shown in Figure 4, the main objectives of the work were a) the computation of the residual rates due to local phenomena and b) the estimation of the contribution of the building consolidation to the phenomenon of subsidence.

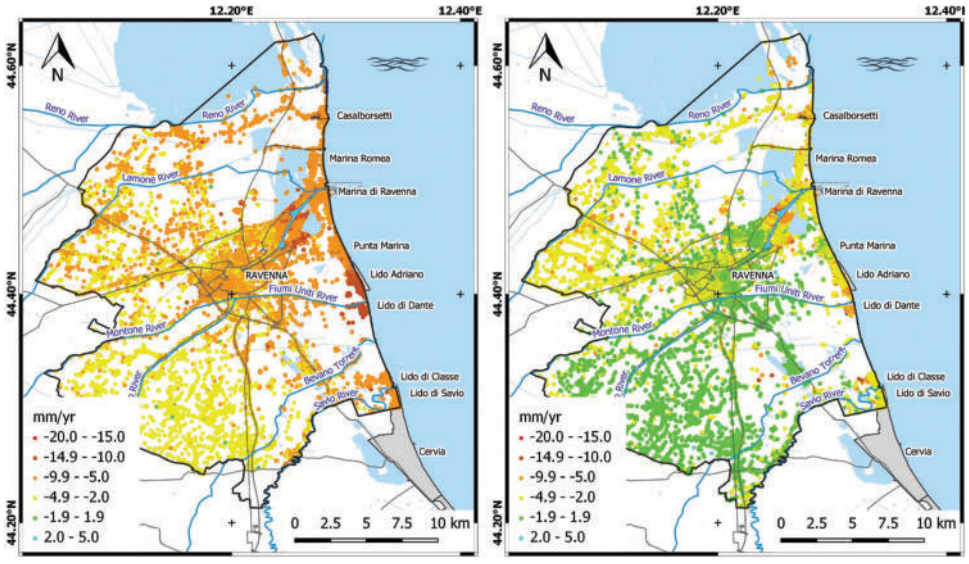

Figure 4. Ascending (left) and descending (right) LOS-oriented velocity maps(mm/yr) of the study area. In the legend, the red color indicates an increase of the range (i.e. a movement away from the satellite).

We define as residual rates the components of the velocity that still remain after the computation and subtraction from ascending and descending slant velocities of the natural component and the temporary effect due to the consolidation processes under building loads; to this aim, the GIS dataset including buildings with the related ages of construction was used. In particular, the purpose of this step is to investigate the possible relationship between the displacements of scatterers representing buildings and the age of construction with successive subtraction of such an effect from the budget of subsidence phenomena and analysis of residual displacements. The workflow in Figure 5 summarizes the proposed approach in which the LOS-oriented velocities for each orbit are used to preserve the full resolution of the SAR data.

However, establishing the spatial relations (e.g. membership or proximity) between the permanent scatterers and building parts producing a response to the radar pulses (i.e. intersection with the building dataset step of Figure 5) is not trivial when data from a moderate resolution (i.e. tens of meters) satellite sensor are used. Furthermore, the geocoding of scatterers over a grid oriented along the azimuth-range directions and errors at few meters level in the spatial positioning of the scatterer make the analysis at building-scale even more difficult. Thus, in order to define the spatial relation between scatterer locations and building shape complemented by descriptive attributes, a preliminary spatial clustering was performed to delineate urban areas characterized by a common age of construction.

The clustering was achieved with a sequence of operations based on vector geometry tools available in QGIS and data attributes. Initially, polygons representing buildings were grouped based on the construction year and intended uses. A buffer with a fixed distance of 2 m was therefore created for all the features in the input layers. Successively, buffers characterized by the same construction year and a particular intended use were dissolved into single multipolygon layers. Finally, spatial criteria were used to assign attributes such as the year of construction and intended use of derived polygons to the descriptive features of single PS. PS falling into more than one polygon or outside any polygon were excluded from the dataset.

The relationship between averaged ascending and descending slant velocities for civil- and industrial-intended uses and year of construction are shown in Figure 6. The steps followed to produce the plot are described in the following. First, the attributes (e.g. the mean LOS velocity and the year of construction) of a building were inherited from each PS belonging to that building. Then, for all the PS of all the buildings with the same year of construction, the mean of the mean velocity is computed, thus, having a single value of velocity representing each year of construction. For the computation of the mean velocity, forty-

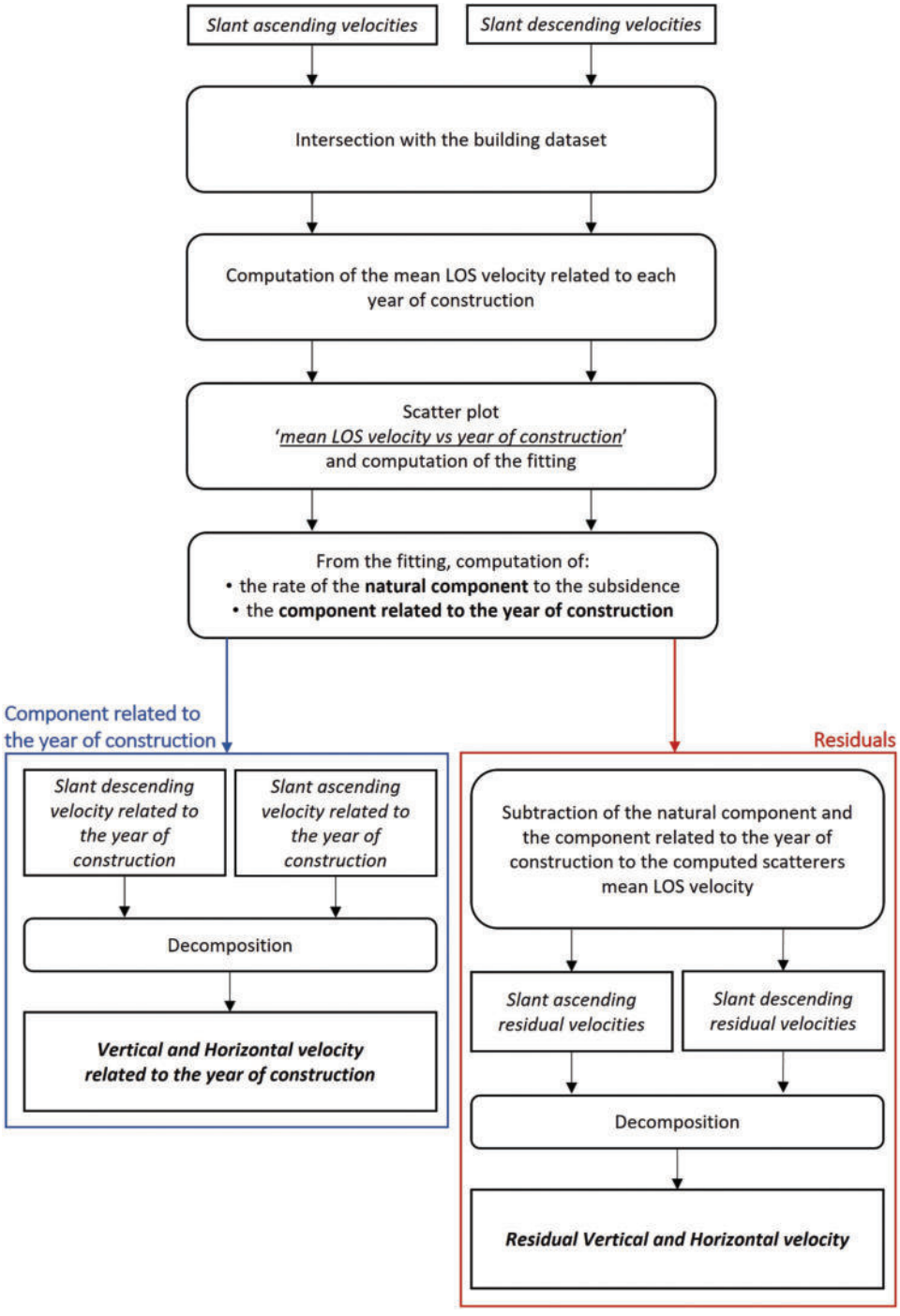

Figure 5. Workflow adopted in the processing of residual slant velocities after subtraction of natural subsidence and displacements due to built areas consolidation.

four thousands and thirty-eight thousands of PS were considered for ascending and descending orbit, respectively. Finally, the mean LOS velocity values versus the years of construction and the fitting of these scatterers were plotted. The color of the scatterers represents the number of PS belonging to buildings constructed in the same year (i.e. the number of PS used to compute the mean velocity related to a given year). The vertical bars in correspondence with the scatterers represent the standard deviation of the computed mean velocity. The fitting function is a piecewise continuous function of the construction year composed by a constant and a parabola branch. The value of the constant,

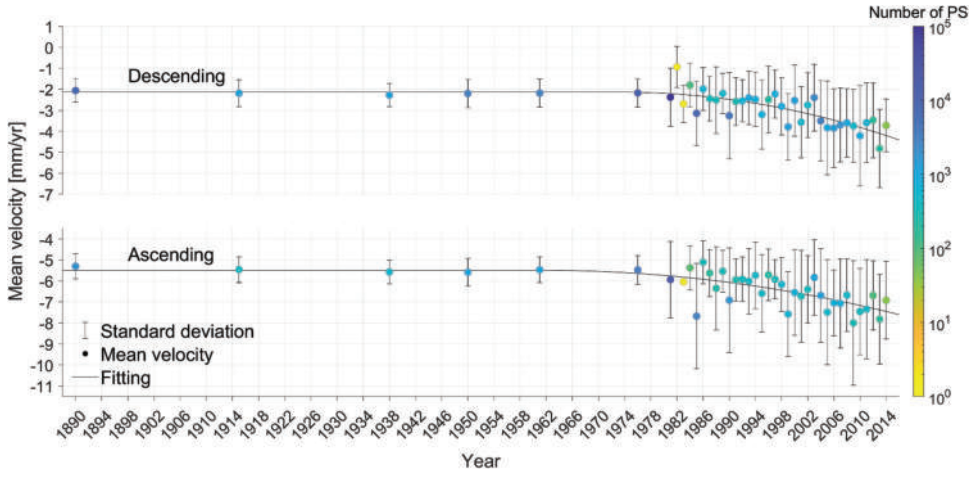

Figure 6. Descending (top) and ascending (bottom) mean LOS velocities of the PS versus the buildings year of construction and their fitting.

the year in which the two functions join and the parabola concavity (i.e. the variables of the fitting function) were obtained solving a constrained non-linear multivariable minimization problem in which the mean squared error between the fitting function itself and the mean velocity values is minimized.

The described procedure was carried out for both the orbits to compute the LOS mean velocity of buildings PS versus the year of construction of the buildings themselves and infer the relation between them.

As can be inferred from Figure 6 for both orbits, the mean LOS velocities of PS belonging to buildings constructed before 1980 have a constant rate. Up to this year, the mean LOS velocity has a constant value of approximately −2 mm/year and −5.5 mm/year for the descending and ascending orbits, respectively. This rate is detected differently by the observing geometry (i.e. from different incidence angles as can be seen from Figure 2) and can be accounted for as the long-period natural component of the subsidence, affecting all the scatterers in the study area. The buildings constructed in the last three decades exhibit increasing values of the mean LOS velocity. For instance, for the descending orbit, as can be seen from the fitting, the mean LOS velocity has a value of −2.2 mm/yr for 1980 and −4.2 mm/yr for 2014. Similarly, for the ascending orbit, the values read by the fitting are −5.8 mm/yr and −7.5 mm/yr for 1980 and 2014, respectively. Figure 6 could be therefore considered as representative of the cumulative subsidence produced by long-term subsidence and time-dependent consolidation processes. Besides the relationship between the slant velocities and the year of construction, an increase of the standard deviations could be observed from the last decades involved. This is likely due to the influence of consolidation processes that, based also on the local stratigraphic setting and construction mode, start to show their effects on more stable long-term displacements. Increasing values of displacements along the slant direction with respect to the year of construction of buildings could be referred to an anthropogenic source due to consolidation processes under the building loads. It contributes to an overestimation of the natural subsidence phenomena or any other deformation processes investigated by the SAR interferometry.

To bring phenomena that deviate from the behavior represented by the fitting curve into evidence, the mean velocity values as read by the fitting curve for each year of construction were subtracted from the corresponding mean LOS velocities of PS. The computed residues are therefore related to local deformation phenomena where long-term displacements and the effect of consolidation processes have been filtered out. The results of the described procedure for both orbits and the corresponding decomposition along the vertical and E-W directions are shown in Figures 7 and 8, respectively.

Residual vertical and horizontal velocities (see Figure 8) show well-defined ground deformation patterns. In the vertical direction, the residual subsidence phenomena other than the natural long-term trend and consolidation processes are located

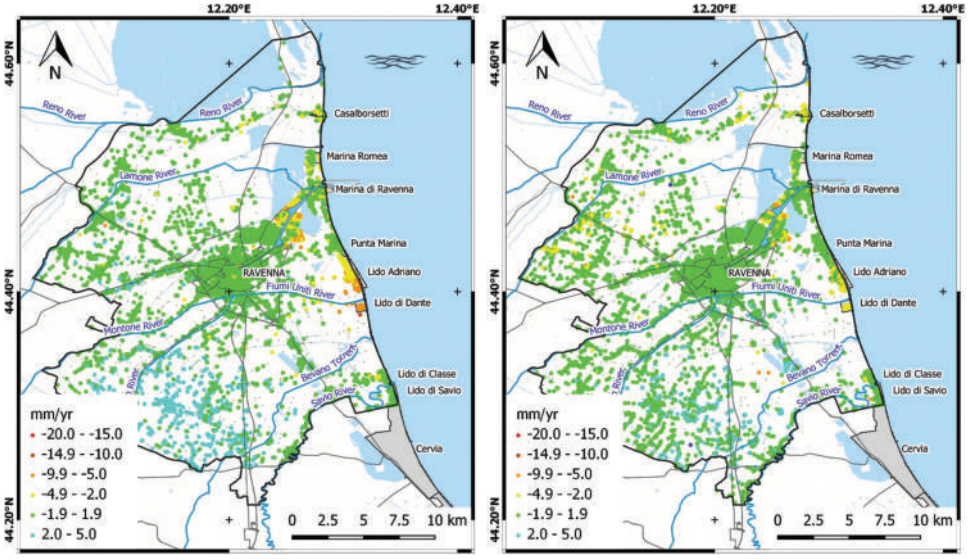

Figure 7. Ascending (left) and descending (right) LOS-oriented residual velocity maps (mm/yr).

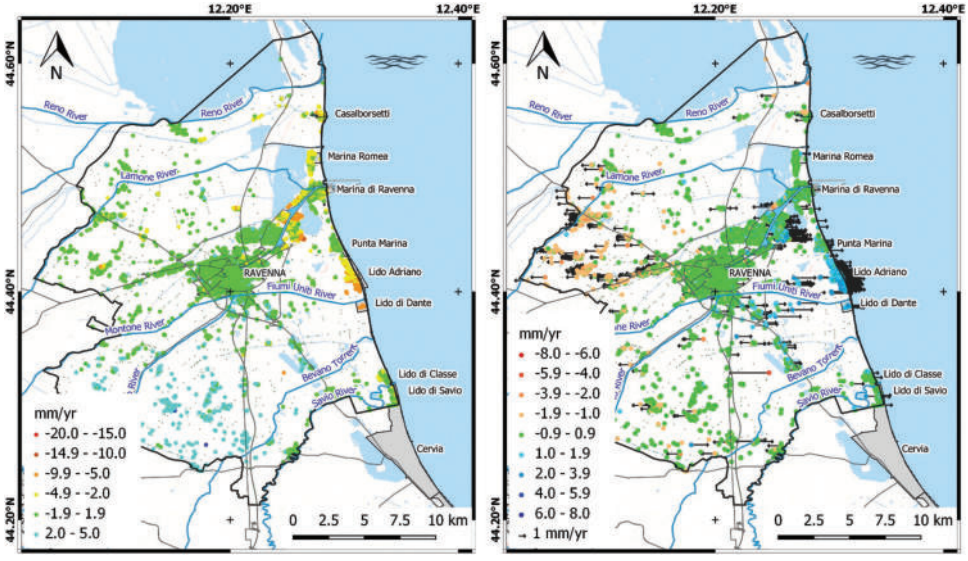

Figure 8. Vertical (left) and horizontal (right) residual velocity maps (mm/yr).

in the coastal villages and industrial areas. As can be seen from Figure 8, the horizontal displacements in the East–West direction show very well delimited spatial pattern mostly located in the coastal village of Lido di Dante and nearby industrial area where velocity field pointing at the East is visible. The possible connection with an offshore gas exploitation activity will be further addressed in the discussion section. Conversely, a wide area located in the central-western portion of the municipality of Ravenna exhibits horizontal velocities oriented in the West direction.

To quantify the effect due to consolidation processes, the mean rate of natural subsidence detected along the LOS directions (i.e. the constant value of the fitting in the plot of Figure 6) was subtracted from the rates detected at any time of construction. Such a procedure enabled the computation of the anthropogenic contribution to the overall subsidence due to consolidation processes. For a better understanding of ground deformation processes due to the mentioned process, the obtained ascending and descending velocities due to anthropogenic processes were decomposed into the corresponding vertical and horizontal components (Figure 9).

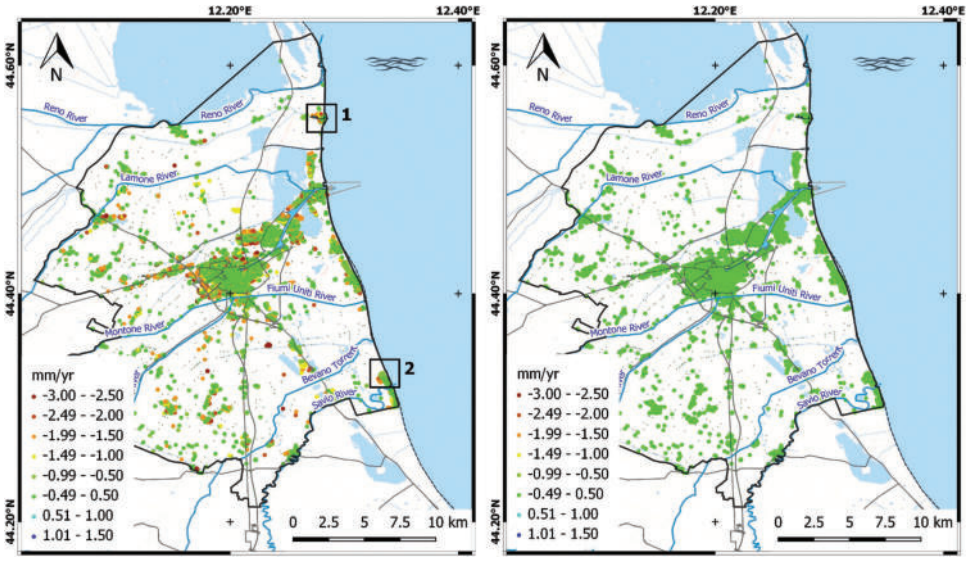

Figure 9. Vertical (left) and horizontal (right) velocity maps related to anthropogenic processes (mm/yr).

In agreement with the hypothesis of consolidation processes, Figure 9 shows a major contribution along the vertical direction, whereas the horizontal component of displacements is very close to zero throughout the area.

For a clearer interpretation about the contribution of consolidation processes to subsidence, Figure 10 shows detailed maps of LOS-oriented displacements over the coastal villages of Casalborsetti and Lido di Classe marked in Figure 9 as area 1 and area 2, respectively.

These areas have been selected to better represent the effect of the consolidation processes over recently built sites. Their limited areal extension allows to represent at detailed scale the LOS-oriented displacements that appear more and more pronounced as the

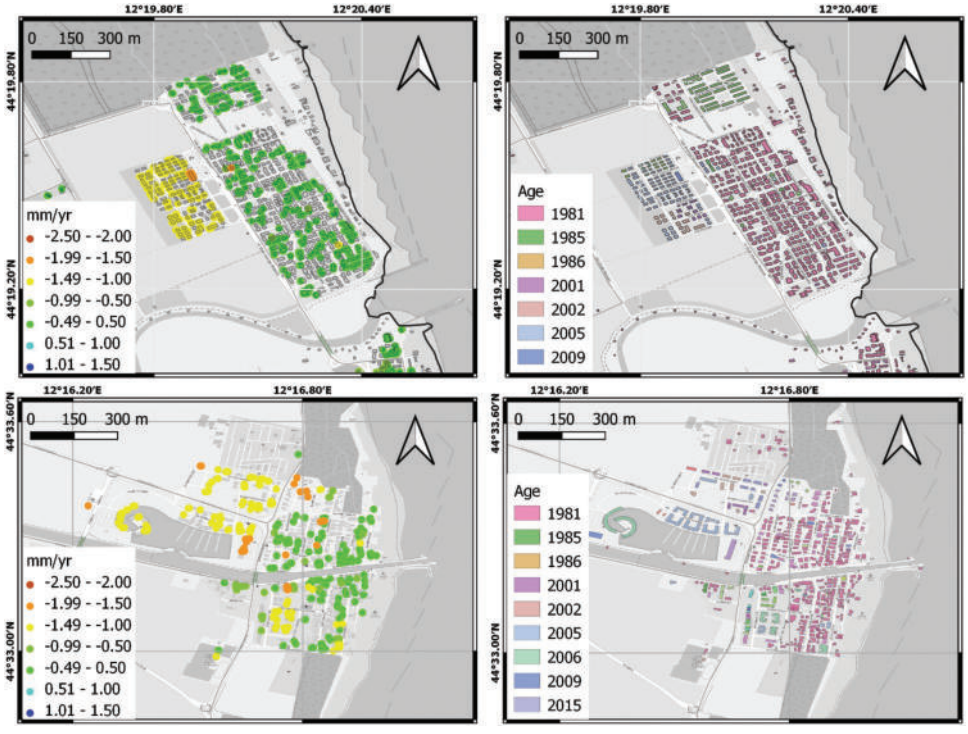

Figure 10. Comparison between the anthropogenic ascending slant velocity maps (left) and the building age (right) for the coastal villages of Lido di Classe (top) and Casalborsetti (bottom).

construction age increases. The effect of anthropogenic processes due to consolidation processes is very well detected once the natural processes have been subtracted. Conversely, the consolidation processes could be masked by natural phenomena when a cumulative effect is observed by the InSAR analysis.

Discussions

Results described in the present paper by the spatial analysis of multi-temporal DInSAR data support a better understating of subsidence phenomena due to natural and anthropogenic causes. The separation of such components allows to quantify and filter out the possible contribution of consolidation processes under building loads occurring over recently settled urban and industrial areas. Potentially, any investigation about ground deformation phenomena based on multi-temporal DInSAR could be strongly biased by such processes. Generally, the consolidation processes are not accounted for and contributions to subsidence of other driving factors could be overestimated. It is the case of DInSAR-based investigations focused to developing areas where consolidation processes could be dominant and related to construction and geotechnical factors (building loads, characteristics of the foundation layer, superficial terrain stratigraphy, geotechnical approaches to structural designing). The relationship between consolidation processes and the age of buildings found in the present paper could further inform on deformation processes occurring at the ground improving the ability to detect displacements due to factors acting at local scale. Moreover, in the investigated area, the consolidations processes seems to be active for more than two decades, a period covering the majority of investigations on subsidence phenomena based on DInSAR methods. It is worth noting that the obtained results are related to the stratigraphic setting of the study area, however, the proposed methodology could be applied in other study areas characterized by different settings and the results will highlight consolidation phenomena of different entities. In this framework, the integration between DInSAR measurements and GIS data, representing buildings with the age of construction, provided a valuable tool in distinguishing consolidation processes after construction from other factors. For instance, Figure 9 shows residual vertical velocities due to such consolidation processes up to 3 mm/yr in the study area, well beyond the mm-level sensitivity of the DInSAR method in the detection of annual rate of displacements. To further improve the reliability of the proposed analysis, the relationship between subsidence rates and age of construction should be established over areas characterized by an homogeneous stratigraphy. It requires additional information as a vector layer representing the superficial stratigraphic layers. In the present paper the study area is characterized by a repeated alternations of coastal and alluvial deposits due to marine transgressive-regressive cyclicity and coastal villages suffering from major subsidence phenomena were settled over well-drained floodplain (Campo, Amorosi, and Vaiani 2017). Such stratigraphic patterns could be considered as representative of the whole coastal areas where major subsidence rates have been detected. However, the presence of different superficial sedimentary bodies (for instance deposits of fluvial channels) may alter the susceptibility to consolidation processes after construction. Future works on the effects of consolidations processes would greatly benefit from improvements in the GIS dataset with regards to the collection, standardization and introduction of parameters from the geotechnic and structural engineering domains. In fact, soil consolidation is potentially affected by several factors such as the building dimensions and weight and the type of foundation. However, foundation design criteria typically limit the maximum soil pressure and/or settlement that can be caused by the building construction. This implies that different buildings realized during the same period have been conceived to cause the same soil pressure and/or settlement. On the contrary, buildings realized at different ages can produce significantly different soil pressure and settlement depending on the limit imposed by the current foundation design criteria and standards. However, such detailed information regarding the buildings is not extensively available in GIS repositories and more simple descriptions must be adopted in their place to predict or assess the consolidation settlements.

The relationship of Figure 6 should be considered as a representative of a general behavior for the dominant stratigraphic setting. However, across the decades the foundation design criteria and the constructive technique of the building (and the typical floor weight with it) evolved and, consequently, the

consolidation processes could reflect the designing approach at the age of construction. For instance, lightweight floors with no concrete slab were typically realized in the 1960s and 1970s, while later in the 1990s concrete slabs became very common. Similarly, wooden roofs have become widespread from the 2000s. All of this means that the age of construction is a synthetic parameter that can represent the several effects affecting the soil consolidation.

As a general remark, we may observe that the consolidation processes could represent the totality of the deformation processes due to postconstruction settlement within areas of recent urbanization where scatterers are mostly represented by roofs. An approach useful in the quantitative assessment of such a contribution should be adopted.

In the present paper, Figure 10 shows LOS-oriented displacements of 2–3 mm/yr over some areas likely due to consolidation settlements of buildings constructed after the year 2000. Approximately, it represents the 20% of the cumulative displacements reported in Figure 4 in the same areas. Such contribution should be removed from the ground deformation processes to better represent subsidence phenomena and the related driving factors.

On the other hand, the subtraction of the long-term rate due to natural subsidence and consolidation processes allows to depict the influence of residual phenomena reported on map of Figure 8 by decomposing velocities into vertical and east–west directions. The analysis of decomposed velocities shows an interesting velocity field in the coastal villages of Lido di Dante and Lido Adriano where subsidence rates up to 10 mm/yr and a dominant eastward displacement up to 3 mm/yr are well depicted. In this area, an offshore exploitation activity of natural gas takes place by a platform installed less than 2 km far from the coastline (see Figure 1 to locate the offshore site ANGA). The rates of ground deformation phenomena in the area have been recently reported by Polcari et al. (2022) whereas, among others, the ability of SAR interferometry to detect the horizontal deformation field produced by a subsidence bowl has been investigated by Samieie-Esfahany et al. (2009).

However, the consolidation processes outlined by the present paper in such an area (up to 3–4 mm/yr) cause an overestimation of the actual subsidence rates due to driving factors other than the consolidation processes themselves. Conversely, the horizontal displacements are not biased by the settlements occurred. The correlation of the horizontal displacement pattern and the offshore gas exploitation activity seems to be evident even though a similar pattern is visible in the industrial area located few km far in the north-western direction where the influence of gas withdrawal should be negligible (see Figure 1). However, the industrial area is also subjected to vertical displacements up to −15 mm/yr over very well delimited sectors occupied by single industrial plants. Unfortunately, the available GIS data do not report the specific industrial activity in the attribute table and such kind of relationship cannot be established. A more detailed description of the industrial activities carried out in any single lot is therefore advised.

In the attempt to filter out the consolidation settlement from the subsidence rates, the use of GNSS as reference must also be addressed. Indeed, when GNSS stations are used to bring DInSAR velocities into a global reference frame, installation of GNSS monuments on recently settled area should be avoided. Otherwise, the contribution of consolidation processes triggered by the building load will be transferred to the totality of PS selected by the multi-temporal interferometric processing. Ancillary subsidence data from topographic leveling could be a valid support in the interpretation of ground deformation. Leveling benchmarks are placed on roads and come from consolidated topographic network; for this reason, vertical displacements derived from leveling measurements are less sensitive to anthropogenic processes of consolidation even though their availability is very limited in most cases.

In the study area, an alternative source of subsidence could be related to groundwater pumping, since 1950s, for irrigation purposes from the multi-layered surficial aquifer (Antonellini et al. 2019). Data provided by ARPAe show a diffuse decrease of the groundwater table from 1990 to 2012 in the area of Ravenna (Antoncecchi 2021). However, in the period of the present investigation, a substantial stability of the groundwater table is reported (ARPAe 2020; Polcari et al. 2022).

Conclusions

The approach proposed in the present paper allows to investigate and separate several contributions to

subsidence phenomena over the municipality of Ravenna (Emilia Romagna, Italy). In particular, consolidation processes after construction were assessed by the use of GIS dataset of the built environment. In the present paper, only few descriptive attributes related to the age of construction and intended uses were adopted in the classification of scatterers, but many others are available and the relationship between rates and sources of subsidence could be further investigated. We demonstrated that the subsidence phenomena could be strongly biased by consolidation processes or ascribed to a different causal factor with an overestimation of its contribution to ground deformation. In the study area, the consolidation processes seem to be active over areas settled in the last 20 years. Thus, such effects should be taken into consideration. For a better interpretation of phenomena, more data about stratigraphy, construction modes and geotechnical factors should be incorporated in the GIS dataset. However, very often such information is not available at very local scale or partially available in a GIS format. To increase the reliability of the proposed analysis, satellite data at higher spatial resolution are advised in addition to a geocoding procedure based on range and azimuth correction after the DEM error assessment. It would improve the spatial linkage between scatterers and GIS information layers with a more reliable analysis of relationship between subsidence phenomena and causal factors.

Acknowledgments

Authors would like to express their thanks to Angelo Galeandro (Eng. PhD) for the development of the decomposition algorithm. The access to Sentinel-1 dataset employed in the present study was performed through the Open Hub of the Copernicus Open Access Hub (scihub.copernicus.eu). The GIS dataset used in this work has been provided by the Municipality of Ravenna.

Disclosure statement

No potential conflict of interest was reported by the author(s).

Funding

The methodology adopted in the present research was partially developed in the frame of the FAR Mission Oriented 2021 Project (Satellite Methods for Structural Monitoring, SM4SM, contract E95F21002900007). The financial support of the University of Modena and Reggio Emilia and the "Fondazione di Modena" is also gratefully acknowledged.

ORCID

Francesco Mancini http://orcid.org/0000-0002-8553-345X

Data availability statement

The data that support the findings of this study are available from the corresponding author, Francesco Mancini, upon reasonable request. https://drive.google.com/drive/u/0/folders/1K2MABCVxrH2hN4h3liTBB3rDBjqjpk-Z

References

Abidin, H. Z., H. Andreas, I. Gumilar, Y. Fukuda, Y. E. Pohan, and T. Deguchi. 2011. "Land Subsidence of Jakarta (Indonesia) and Its Relation with Urban Development." *Natural Hazards* 59 (3): 1753–1771. doi:10.1007/s11069-011-9866-9.

Antoncecchi, I., F. Ciccone, G. Rossi, G. Agate, F. Colucci, F. Moia, and L. Petracchini. 2021. "Soil Deformation Analysis through Fluid-Dynamic Modelling and DInSAR Measurements: A Focus on Groundwater Withdrawal in the Ravenna Area (Italy)." *Bollettino Di Geofisica Teorica Ed Applicata* 62 (2). doi:10.4430/bgta0350.

Antonellini, M., B. M. S. Giambastiani, N. Greggio, L. Bonzi, L. Calabrese, P. Luciani, L. Perini, and P. Severi. 2019. "Processes Governing Natural Land Subsidence in the Shallow Coastal Aquifer of the Ravenna Coast, Italy." *Catena* 172: 76–86. doi:10.1016/j.catena.2018.08.019.

ARPAe. 2018. *Rilievo della subsidenza nella pianura emiliano-romagnola seconda fase*. ARPAe. https://ambiente.regione.emilia-romagna.it/it/acque/approfondimenti/documenti/rilievo-della-subsidenza-nella-pianura-emiliano-romagnola/seconda-fase

ARPAe. 2020. *Valutazione dello stato delle acque sotterranee 2014-2019*. ARPAe. https://ambiente.regione.emilia-romagna.it/it/acque/approfondimenti/normativa/allegato-3-report_acque_sotterranee_2014-2019_d.pdf

Barra, A., C. Reyes-Carmona, G. Herrera, J. P. Galve, L. Solari, R. M. Mateos, J. M. Azañón, et al. 2022. "From Satellite Interferometry Displacements to Potential Damage Maps: A Tool for Risk Reduction and Urban Planning." *Remote Sensing of Environment* 282 (December): 113294. doi:10.1016/j.rse.2022.113294.

Bekaert, D. P. S., A. Hooper, and T. J. Wright. 2015. "A Spatially Variable Power Law Tropospheric Correction Technique for InSAR Data." *Journal of Geophysical Research: Solid Earth* 120 (2): 1345–1356. doi:10.1002/2014JB011558.

Bekaert, D. P. S., R. J. Walters, T. J. Wright, A. J. Hooper, and D. J. Parker. 2015. "Statistical Comparison of InSAR Tropospheric Correction Techniques." *Remote Sensing of Environment* 170: 40–47. doi:10.1016/j.rse.2015.08.035.

Berardino, P., G. Fornaro, R. Lanari, and E. Sansosti. 2002. "A New Algorithm for Surface Deformation Monitoring Based on Small Baseline Differential SAR Interferograms." *IEEE Transaction on Geoscience and Remote Sensing* 40 (11): 2375–2383. doi:10.1109/TGRS.2002.803792.

Bertoni, W., G. Brighenti, G. Gambolati, G. Ricceri, and F. Vuillermin. 1995. "Land Subsidence Due to Gas Production in the On-and Offshore Natural Gas Fields of the Ravenna Area, Italy." In *IAHS Publications-Series of Proceedings and Reports-International Association of Hydrological Sciences*, The Hague, NL, 234:13–20.

Bitelli, G., F. Bonsignore, I. Pellegrino, and L. Vittuari. 2015. "Evolution of the Techniques for Subsidence Monitoring at Regional Scale: The Case of Emilia-Romagna Region (Italy)." *Proceeding of the IAHS 2015* 372: 315. doi:10.5194/piahs-372-315-2015.

Bonetti, J., F. Del Bianco, L. Schippa, A. Polonia, G. Stanghellini, N. Cenni, S. Draghetti, F. Marabini, and L. Gasperini. 2022. "Anatomy of Anthropically Controlled Natural Lagoons through Geophysical, Geological, and Remote Sensing Observations: The Valli Di Comacchio (NE Italy) Case Study." *Remote Sensing* 14 (4): 987. doi:10.3390/rs14040987.

Bui, L. K., P. V. V. Le, P. D. Dao, N. Quoc Long, H. V. Pham, H. Ha Tran, and L. Xie. 2021. "Recent Land Deformation Detected by Sentinel-1A InSAR Data (2016–2020) over Hanoi, Vietnam, and the Relationship with Groundwater Level Change." *GIScience & Remote Sensing* 58 (2): 161–179. Taylor & Francis. doi:10.1080/15481603.2020.1868198.

Campo, B., A. Amorosi, and S. C. Vaiani. 2017. "Sequence Stratigraphy and Late Quaternary Paleoenvironmental Evolution of the Northern Adriatic Coastal Plain (Italy)." *Palaeogeography, Palaeoclimatology, Palaeoecology* 466: 265–278. doi:10.1016/j.palaeo.2016.11.016.

Carminati, E., C. Doglioni, and D. Scrocca. 2003. "Apennines Subduction-Related Subsidence of Venice (Italy)." *Geophysical Research Letters* 30 (13): 50–51. doi:10.1029/2003GL017001.

Carminati, E., and G. Martinelli. 2002. "Subsidence Rates in the Po Plain, Northern Italy: The Relative Impact of Natural and Anthropogenic Causation." *Engineering Geology* 66 (3–4): 241–255. doi:10.1016/S0013-7952(02)00031-5.

Casu, F., M. Manzo, and R. Lanari. 2006. "A Quantitative Assessment of the SBAS Algorithm Performance for Surface Deformation Retrieval from DInSAR Data." *Remote Sensing of Environment* 102 (3): 195–210. doi:10.1016/j.rse.2006.01.023.

Cerenzia, I., D. Putero, F. Bonsignore, G. Galassi, M. Olivieri, and G. Spada. 2016. "Historical and Recent Sea Level Rise and Land Subsidence in Marina Di Ravenna, Northern Italy." *Annals of Geophysics* 59 (5): 0546. doi:10.4401/ag-7022.

Chen, B., H. Gong, X. Li, K. Lei, Y. Ke, G. Duan, and C. Zhou. 2015. "Spatial Correlation between Land Subsidence and Urbanization in Beijing, China." *Natural Hazards* 75 (3): 2637–2652. doi:10.1007/s11069-014-1451-6.

Chen, W. F., and J. Y. Richard Liew. 2002. *The Civil Engineering Handbook*.2nd ed. Boca Raton: CRC Press. doi:10.1201/9781420041217.

Cian, F., J. M. Delgado Blasco, and L. Carrera. 2019. "Sentinel-1 for Monitoring Land Subsidence of Coastal Cities in Africa Using PSInSAR: A Methodology Based on the Integration of SNAP and StaMPS." *Geosciences* 9 (3): 124. doi:10.3390/geosciences9030124.

Crosetto, M., O. Monserrat, M. Cuevas-González, N. Devanthéry, and B. Crippa. 2016. "Persistent Scatterer Interferometry: A Review." *ISPRS Journal of Photogrammetry and Remote Sensing* 115 (May): 78–89. doi:10.1016/j.isprsjprs.2015.10.011.

Dang, V. K., C. Doubre, C. Weber, N. Gourmelen, and F. Masson. 2014. "Recent Land Subsidence Caused by the Rapid Urban Development in the Hanoi Region (Vietnam) Using ALOS InSAR Data." *Natural Hazards and Earth System Sciences* 14 (3): 657–674. doi:10.5194/nhess-14-657-2014.

Delgado Blasco, J. M., M. Foumelis, C. Stewart, and A. Hooper. 2019. "Measuring Urban Subsidence in the Rome Metropolitan Area (Italy) with Sentinel-1 SNAP-StaMPS Persistent Scatterer Interferometry." *Remote Sensing* 11 (2): 129. Multidisciplinary Digital Publishing Institute. doi:10.3390/rs11020129.

Del Soldato, M., G. Farolfi, A. Rosi, F. Raspini, and N. Casagli. 2018. "Subsidence Evolution of the Firenze–Prato–Pistoia Plain (Central Italy) Combining PSI and GNSS Data." *Remote Sensing* 10 (7): 1146. doi:10.3390/rs10071146.

Farolfi, G., S. Bianchini, and N. Casagli. 2019. "Integration of GNSS and Satellite InSAR Data: Derivation of Fine-Scale Vertical Surface Motion Maps of Po Plain, Northern Apennines, and Southern Alps, Italy." *IEEE Transactions on Geoscience and Remote Sensing* 57 (1): 319–328. doi:10.1109/TGRS.2018.2854371.

Ferretti, A., A. Fumagalli, F. Novali, C. Prati, F. Rocca, and A. Rucci. 2011. "A New Algorithm for Processing Interferometric data-stacks: SqueeSAR." *IEEE Transaction on Geoscience and Remote Sensing* 49 (9): 3460–3470. doi:10.1109/TGRS.2011.2124465.

Ferretti, A., C. Prati, and F. Rocca. 2000. "Nonlinear Subsidence Rate Estimation Using Permanent Scatterers in Differential SAR Interferometry." *IEEE Transaction on Geoscience and Remote Sensing* 38 (5): 2202–2212. doi:10.1109/36.868878.

Ferretti, A., C. Prati, and F. Rocca. 2001. "Permanent Scatterers in SAR Interferometry." *IEEE Transaction on Geoscience and Remote Sensing* 39 (1): 8–20. doi:10.1109/36.898661.

Fiaschi, S., S. Tessitore, R. Bonì, D. Martire, V. Achilli, S. Borgstrom, A. Ibrahim, et al. 2017. "From ERS-1/2 to Sentinel-1: Two Decades of Subsidence Monitored through A-DInSAR Techniques in the Ravenna Area (Italy)." *GIScience & Remote Sensing* 54 (3): 305–328. doi:10.1080/15481603.2016.1269404.

Gabriel, A. K., R. M. Goldstein, and H. A. Zebker. 1989. "Mapping Small Elevation Changes over Large Areas: Differential Radar Interferometry." *Journal of Geophysical Research: Solid Earth* 94 (B7): 9183–9191. doi:10.1029/JB094iB07p09183.

Gambolati, G., and P. Teatini. 1998. "Numerical Analysis of Land Subsidence Due to Natural Compaction of the Upper Adriatic Sea Basin." In *CENAS*, 103–131. Dordrecht: Springer. doi:10.1007/978-94-011-5147-4_5.

Ghorbanzadeh, O., H. Rostamzadeh, T. Blaschke, K. Gholaminia, and J. Aryal. 2018. "A New GIS-Based Data Mining Technique Using an Adaptive Neuro-Fuzzy Inference System (ANFIS) and k-Fold Cross-Validation Approach for Land Subsidence Susceptibility Mapping." *Natural Hazards* 94 (2): 497–517. doi:10.1007/s11069-018-3449-y.

Hanssen, R. F. 2001. *Radar Interferometry: Data Interpretation and Error Analysis*. Dordrecht, The Netherlands: Springer Science & Business Media.

Hooper, A., D. Bekaert, E. Hussain, and K. Spaans. 2018. *StaMPS/MTI Manual (Version 4.1b)*. Leeds, UK: University of Leeds. https://homepages.see.leeds.ac.uk/~earahoo/stamps/

Hooper, A., D. Bekaert, K. Spaans, and M. Arıkan. 2012. "Recent Advances in SAR Interferometry Time Series Analysis for Measuring Crustal Deformation." *Tectonophysics* 514: 1–13. doi:10.1016/j.tecto.2011.10.013.

Hooper, A., P. Segall, and H. Zebker. 2007. "Persistent Scatterer InSAR for Crustal Deformation Analysis, with Application to Volcán Alcedo, Galápagos." *Journal of Geophysical Research: Solid Earth* 112 (B07407): 19. doi:10.1029/2006JB004763.

Hooper, A., H. Zebker, P. Segall, and B. Kampes. 2004. "A New Method for Measuring Deformation on Volcanoes and Other Natural Terrains Using InSAR Persistent Scatterers." *Geophysical Research Letters* 31 (23): 23. doi:10.1029/2004GL021737.

Ketelaar, G., H. Bähr, S. Liu, H. Piening, W. Veen, R. Hanssen, and S. Samiei-Esfahany. 2020. "Integrated Monitoring of Subsidence Due to Hydrocarbon Production: Consolidating the Foundation." In *Proceedings of the International Association of Hydrological Sciences*, Delft, NL, 382:117–123. doi: 10.5194/piahs-382-117-2020.

Lanari, R., O. Mora, M. Manunta, J. J. Mallorquí, P. Berardino, and E. Sansosti. 2004. "A small-baseline Approach for Investigating de-formations on full-resolution Differential SAR Interferograms." *IEEE Transaction on Geoscience and Remote Sensing* 42 (7): 1377–1386. doi:10.1109/TGRS.2004.828196.

Li, F., G. Liu, H. Gong, B. Chen, and C. Zhou. 2022. "Assessing Land Subsidence-Inducing Factors in the Shandong Province, China, by Using PS-InSAR Measurements." *Remote Sensing* 14 (12): 2875. doi:10.3390/rs14122875.

Lyu, M., Y. Ke, L. Guo, X. Li, L. Zhu, H. Gong, and C. Constantinos. 2020. "Change in Regional Land Subsidence in Beijing after South-to-North Water Diversion Project Observed Using Satellite Radar Interferometry." *GIScience & Remote Sensing* 57 (1): 140–156. Taylor & Francis. doi:10.1080/15481603.2019.1676973.

Macchiarulo, V., P. Milillo, C. Blenkinsopp, and G. Giardina. 2022. "Monitoring Deformations of Infrastructure Networks: A Fully Automated GIS Integration and Analysis of InSAR Time-Series." *Structural Health Monitoring* 21 (4): 1849–1878. SAGE Publications. doi:10.1177/14759217211045912.

Mancini, F., F. Grassi, and N. Cenni. 2021. "A Workflow Based on SNAP–StaMPS Open-Source Tools and GNSS Data for PSI-Based Ground Deformation Using Dual-Orbit Sentinel-1 Data: Accuracy Assessment with Error Propagation Analysis." *Remote Sensing* 13 (4): 753. doi:10.3390/rs13040753.

Polcari, M., V. Secreti, L. Anderlini, M. Albano, M. Palano, E. Serpelloni, G. Pezzo, E. Trasatti, and G. Pezzo. 2022. "Multi-Technique Geodetic Detection of Onshore and Offshore Subsidence along the Upper Adriatic Sea Coasts." *International Journal of Applied Earth Observation and Geoinformation* 108: 102756. doi:10.1016/j.jag.2022.102756.

Qin, Y., and D. Perissin. 2015. "Monitoring Ground Subsidence in Hong Kong via Spaceborne Radar: Experiments and Validation." *Remote Sensing* 7 (8): 10715–10736. doi:10.3390/rs70810715.

Qiu, Z., O. Monserrat, M. Crosetto, V. Krishnakumar, and L. Zhou. 2021. "An Innovative Extraction Methodology of Active Deformation Areas Based on Sentinel-1 SAR Dataset: The Catalonia Case Study." *International Journal of Remote Sensing* 42 (16): 6228–6244. Taylor & Francis. doi:10.1080/01431161.2021.1937749.

Radman, A., M. Akhoondzadeh, and B. Hosseiny. 2021. "Integrating InSAR and Deep-Learning for Modeling and Predicting Subsidence over the Adjacent Area of Lake Urmia, Iran." *GIScience & Remote Sensing* 58 (8): 1413–1433. Taylor & Francis. doi:10.1080/15481603.2021.1991689.r.

Samieie-Esfahany, S., R. Hanssen, K. Thienen-Visser, and A. Muntendam-Bos. 2009. "On the Effect of Horizontal Deformation on InSAR Subsidence Estimates." In *Proceedings of the Fringe 2009 Workshop*. Frascati, Italy.

Samsonov, S., N. d'Oreye, and B. Smets. 2013. "Ground Deformation Associated with Post-Mining Activity at the French–German Border Revealed by Novel InSAR Time Series Method." *International Journal of Applied Earth Observation and Geoinformation* 23 (August): 142–154. doi:10.1016/j.jag.2012.12.008.

Scivetti, N., P. Marcos, M. E. Prieto, C. Pavón Pivetta, L. Benedini, A. J. Stremel, M. E. Bahía, A. Bilmes, and S. Richiano. 2021. "Geomorphological and Anthropic Impacts over Land Surface Displacements: Application of DInSAR Technique to the Case of Bahía Blanca City, Argentina." *Geocarto International* : 1–20. Taylor & Francis. doi:10.1080/10106049.2021.1974960.

Simeoni, U., U. Tessari, C. Corbau, O. Tosatto, P. Polo, and P. Teatini. 2017. "Impact of Land Subsidence Due to Residual Gas Production on Surficial Infrastructures: The Dosso Degli Angeli Field Study (Ravenna, Northern Italy)." *Engineering Geology* 229: 1–12. doi:10.1016/j.enggeo.2017.09.008.

Solari, L., A. Ciampalini, F. Raspini, S. Bianchini, and S. Moretti. 2016. "PSInSAR Analysis in the Pisa Urban Area (Italy): A Case Study of Subsidence Related to Stratigraphical Factors and Urbanization." *Remote Sensing* 8 (2): 120. doi:10.3390/rs8020120.

Stramondo, S., F. Bozzano, F. Marra, U. Wegmuller, F. R. Cinti, M. Moro, and M. Saroli. 2008. "Subsidence Induced by Urbanisation in the City of Rome Detected by Advanced InSAR Technique and Geotechnical Investigations." *Remote*

Sensing of Environment 112 (6): 3160–3172. doi:10.1016/j.rse.2008.03.008.

Stramondo, S., M. Saroli, C. Tolomei, M. Moro, F. Doumaz, A. Pesci, F. Loddo, P. Baldi, and E. Boschi. 2007. "Surface Movements in Bologna (Po Plain - Italy) Detected by Multitemporal DInSAR." *Remote Sensing of Environment* 110 (3): 304–316. doi:10.1016/j.rse.2007.02.023.

Sytnik, O., and F. Stecchi. 2014. "Disappearing Coastal Dunes: Tourism Development and Future Challenges, a Case Study from Ravenna, Italy." *Journal of Coast Conservation* 19 (5): 715–727. doi:10.1007/s11852-014-0353-9.

Tang, Y. Q., Z. D. Cui, J. X. Wang, C. Lu, and X. X. Yan. 2008. "Model Test Study of Land Subsidence Caused by High-Rise Building Group in Shanghai." *Bulletin of Engineering Geology and the Environment* 67 (2): 173–179. doi:10.1007/s10064-008-0121-x.

Teatini, P., M. Ferronato, G. Gambolati, W. Bertoni, and M. Gonella. 2005. "A Century of Land Subsidence in Ravenna, Italy." *Environmental Geology* 47 (6): 831–846. doi:10.1007/s00254-004-1215-9.

Teatini, P., M. Ferronato, G. Gambolati, and M. Gonella. 2006. "Groundwater Pumping and Land Subsidence in the Emilia-Romagna Coastland, Italy: Modeling the past Occurrence and the Future Trend." *Water Resources Research* 42 (1): W01406. doi:10.1029/2005WR004242.

Teatini, P., L. Tosi, and T. Strozzi. 2011. "Quantitative Evidence that Compaction of Holocene Sediments Drives the Present Land Subsidence of the Po Delta, Italy." *Journal of Geophysical Research: Solid Earth* 116 (B8). doi:10.1029/2010JB008122.

Tomás, R., J. I. Pagán, J. A. Navarro, M. Cano, J. L. Pastor, A. Riquelme, M. Cuevas-González, et al. 2019. "Semi-Automatic Identification and Pre-Screening of Geological–Geotechnical Deformational Processes Using Persistent Scatterer Interferometry Datasets." *Remote Sensing* 11 (14): 1675. doi:10.3390/rs11141675.

Tosi, L., P. Teatini, and T. Strozzi. 2013. "Natural versus Anthropogenic Subsidence of Venice." *Scientific. Reports* 3 (1): 2710. doi:10.1038/srep02710.

Van Leijen, F. J., H. Marel, and R. F. Hanssen. 2021. "Towards the Integrated Processing of Geodetic Data." In *2021 IEEE International Geoscience and Remote Sensing Symposium IGARSS*, 3995–3998. Brussels, Belgium: IEEE. doi: 10.1109/IGARSS47720.2021.9554887.

Wang, S., G. Zhang, Z. Chen, H. Cui, Y. Zheng, Z. Xu, and Q. Li. 2022. "Surface Deformation Extraction from Small Baseline Subset Synthetic Aperture Radar Interferometry (SBAS-InSAR) Using Coherence-Optimized Baseline Combinations." *GIScience & Remote Sensing* 59 (1): 295–309. Taylor & Francis. doi:10.1080/15481603.2022.2026639.

Xu, Y. S., L. Ma, Y. J. Du, and S. L. Shen. 2012. "Analysis of Urbanisation-Induced Land Subsidence in Shanghai." *Natural Hazards* 63 (2): 1255–1267. doi:10.1007/s11069-012-0220-7.

Zebker, H. A., and J. Villasenor. 1992. "Decorrelation in Interferometric Radar Echoes." *IEEE Transaction on Geoscience and Remote Sensing* 30 (5): 950–959. doi:10.1109/36.175330.